

CFOSAT 2nd International Science team Meeting

# CFOSAT and Sentinel-1 intercomparisons for Significant Wave Height measurements

March 2021  
Visio meeting

LOPS SIAM(1) - University of Hawaii(2)

Antoine Grouazel(1), Justin Stopa(2), Alexis Mouche(1) and Bertrand Chapron(1)

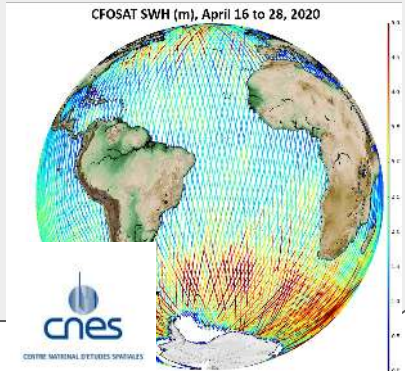


# Abstract

This study provides a comparison between CFOSAT and Sentinel-1 wave measurements. Recently, new methods have been developed to analyze Sentinel-1 C-band SAR data acquired over open ocean in the so-called Wave Mode for estimating the significant wave height [Quach et al., 2020] and for classifying the images with respect to the dominant geophysical parameter [Wang et al., 2019]. These two informations are systematically derived from Sentinel-1 A and Sentinel-1 B measurements collocated with CFOSAT. The significant wave height as measured by CFOSAT and Sentinel-1 are then compared. Performances (RMSE, correlation and bias) are presented and analyzed with respect to geographical location, wind regimes and dominant geophysical signatures captured by the SAR. Emphasis on complex situations and/or inconsistent cases are discussed.

# Datasets

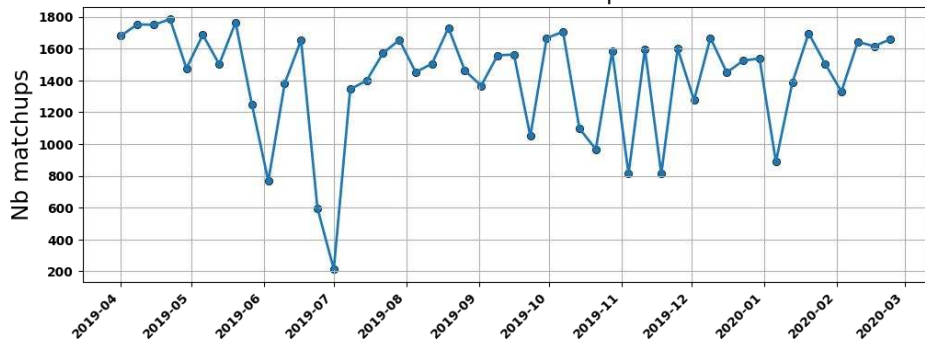
CFOSAT SWIM Ku-band spectrometer nadir beam Level-2 CWWIC at box 70 x 90 km resolution. Adaptive retracking algorithm.



Aviso altimetry courtesy.

CFOSAT and Sentinel-1 units present heliosynchronous orbits that offer very long matchups opportunities. The time criteria used for this study is +/-2 hours and 100 km radius.

Count nb colocs SWIM WV per week

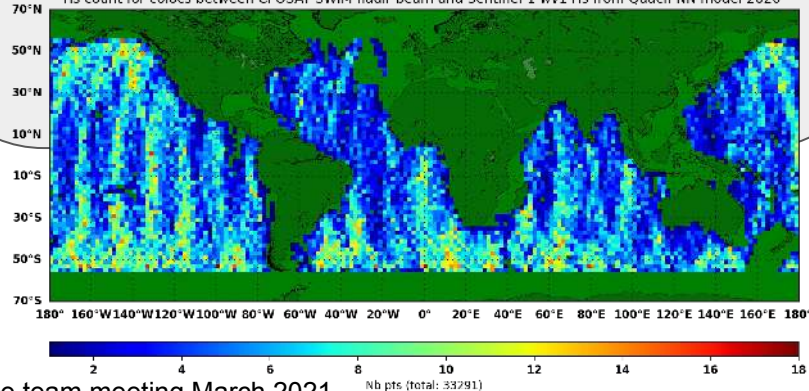


Sentinel-1 A & B WV C-band SAR. Leapfrog acquisitions 24° and 37° incidence angle every 200 km (~ 3 seconds ) at global scale, Hs dataset build using Quach et al 2020 NN model develop at University of Hawaii and operated at IFREMER in the frame of 2 ESA projects:

- Sentinel-1 MPC (Mission Performance Center)
- CCI Sea state (algorithm selected for official CCI datasets)



Hs count for colocs between CFOSAT SWIM nadir beam and Sentinel-1 wv1 Hs from Quach NN model 2020

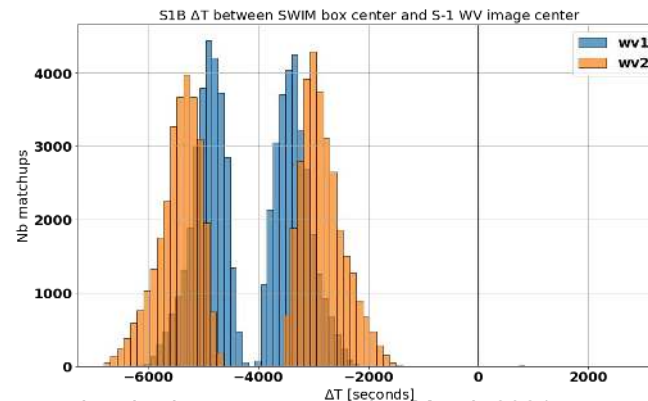
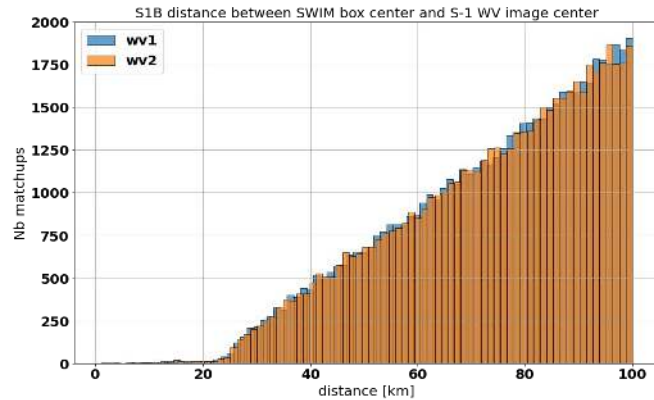
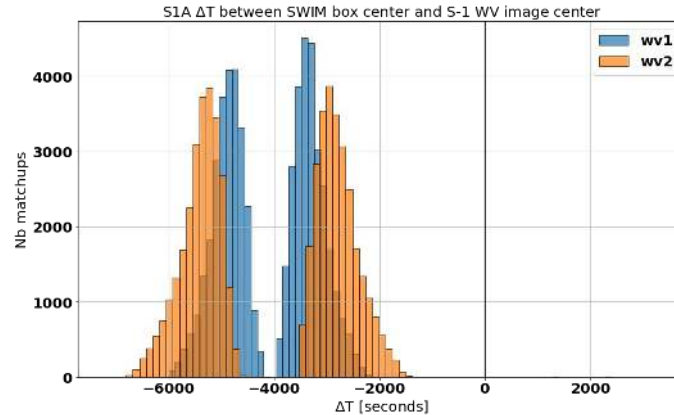
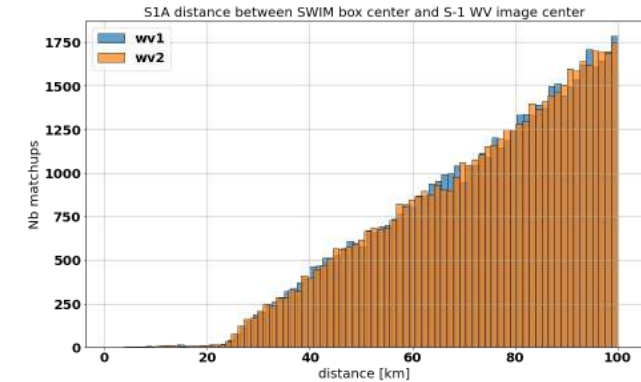


# Matchups between SWIM and Sentinel-1 WV

$\Delta T$  : +/-2 hours

$\Delta$ geographic: 100 km

S1A and S1B are matching CFOSAT 100 km radius with 1 or 2 hours advance .



# SAR NN model to get Hs from WV cross spectra: QUACH *et al* 2020

## Deep Learning for Predicting Significant Wave Height From Synthetic Aperture Radar

Brandon Quach<sup>1</sup>, Yannik Glaser<sup>2</sup>, Justin Edward Stopa<sup>3</sup>, Alexis Aurelien Mouche<sup>4</sup>, and Peter Sadowski<sup>5</sup>

**Abstract**—The Sentinel-1 satellites equipped with synthetic aperture radars (SARs) provide near-global coverage of the world's oceans every six days. We create a data set of collocations between SAR and altimetric satellites and investigate the use of deep learning to predict significant wave height from SAR. While previous models for predicting geophysical quantities from SAR rely heavily on feature-engineering, our approach learns directly from low-level image cross-spectra. Training on collocations from 2015 to 2017, we demonstrate on test data from 2018 that deep learning reduces the state-of-the-art root mean squared error by 50%, from 0.6 to 0.3 m when compared to altimetric data. Furthermore, we isolate the contributions of different features to the model performance.

**Index Terms**—CWAVE, deep learning, machine learning, neural networks, Sentinel-1, significant wave height, synthetic aperture radar (SAR).

### I. INTRODUCTION

SYNTHETIC aperture radar (SAR) enables us to measure submesoscale phenomena with unprecedented coverage, resolution, and frequency. By measuring the backscatter from the ocean surface, SAR captures information about ocean swells and sea surface roughness at high spatial resolutions (<10 m) [1], from which many oceanic, atmospheric, and biologic phenomena can be identified [2]. The two Sentinel-1 satellites of the European Space Agency (ESA) take regular SAR measurements of the ocean surface, together covering the entire globe every six days [3], and have already accumulated more than 600 TB of level-1 (L1) wave mode data. However, in order to take full advantage of this technology and the torrent of data being produced, new methods are needed to extract useful information from the high-dimensional measurements.

Sea state information extracted from SAR has been instrumental in understanding swell decay [1], [4], [5], improving swell propagation in numerical models [6], and predicting swell amplitudes and arrival times by assimilation into numerical models [7]. SAR can also be used to estimate extreme

Manuscript received February 14, 2020; revised May 22, 2020; accepted June 8, 2020. (Corresponding author: Justin Edward Stopa.)

Brandon Quach is with the Computing and Mathematical Sciences Department, California Institute of Technology, Pasadena, CA 91125-0002 USA, and also with the Information and Computer Sciences Department, University of Hawaii at Manoa, Honolulu, HI 96822 USA.

Justin Edward Stopa is with Ocean Engineering Department, University of Hawaii at Manoa, Honolulu, HI 96822 USA (e-mail: stopa@hawaii.edu).

Alexis Aurelien Mouche is with the Univ. Brest, CNRS, IRD, IFREMER, Laboratoire d'Océanographie Physique et Spatiale, ODPSS, IRDUM, 29200 Brest, France.

Color versions of one or more of the figures in this article are available online at <http://dx.doi.org/10.1109/TGRS.2020.3003839>.

Digital Object Identifier 10.1109/TGRS.2020.3003839

0196-2892 © 2020 IEEE. Personal use is permitted, but republication/redistribution requires IEEE permission. See [http://www.ieee.org/publications\\_standards/publications\\_standards.html](http://www.ieee.org/publications_standards/publications_standards.html) for more information.

sea states in extra-tropical and tropical cyclones [8]–[10]. A geophysical quantity of particular interest is the *significant wave height*,  $H_s$ , defined as the mean of the top third of a wave height distribution, and estimating  $H_s$  from SAR has immediate practical uses in alerting ships to dangerously large waves. Traditional “inverse” algorithms for inferring  $H_s$  from SAR are slow and perform poorly in windy conditions typical of most storms [11], [12] because of the complex nonlinear mechanism involved in the image synthesis when observing moving scenes. As a result, several recent studies have focused on data-driven statistical models [8]–[10], [13].

Previous data-driven approaches for predicting  $H_s$  from SAR used small data sets of buoy observations as targets for training (<5000 examples) [14]–[16], or numerical models of global wave generation such as WAVEWATCH3 [8], [10], [13], [17]. The current state-of-the-art method uses a neural network trained on the latter, and predicts  $H_s$  with 0.6-m root mean squared error (RMSE) [10]. However, the WAVEWATCH3 targets are only an *estimate* of  $H_s$  and are known to be unreliable in high sea states [18]–[20].

Furthermore, the neural network in [10] relies on a reduced representation of the modulation cross-spectra: a set of 22 engineered features known as CWAVE [13]. Such dimensionality-reduction methods can be very useful, but often come at the cost of discarding relevant information. We hypothesize that the SAR image modulation spectra contains *additional information* about  $H_s$  that is lost by the CWAVE dimensionality-reduction step. We propose to *learn* the relevant intermediate data representations using deep learning with artificial neural networks, similar to what has been done in other fields from computer vision [21] to high-energy physics [22]–[24].

In this work, we address both limitations of current data-driven  $H_s$  prediction models. First, we create a data set containing *direct observations* of ocean wave heights by identifying 750,000 collocations of SAR and altimetric satellites. Second, we train a statistical model to extract information directly from low-level SAR image spectra using deep learning. Finally, we analyze the importance of the different inputs to this model, and its performance in different settings.

### II. DATA AND METHODS

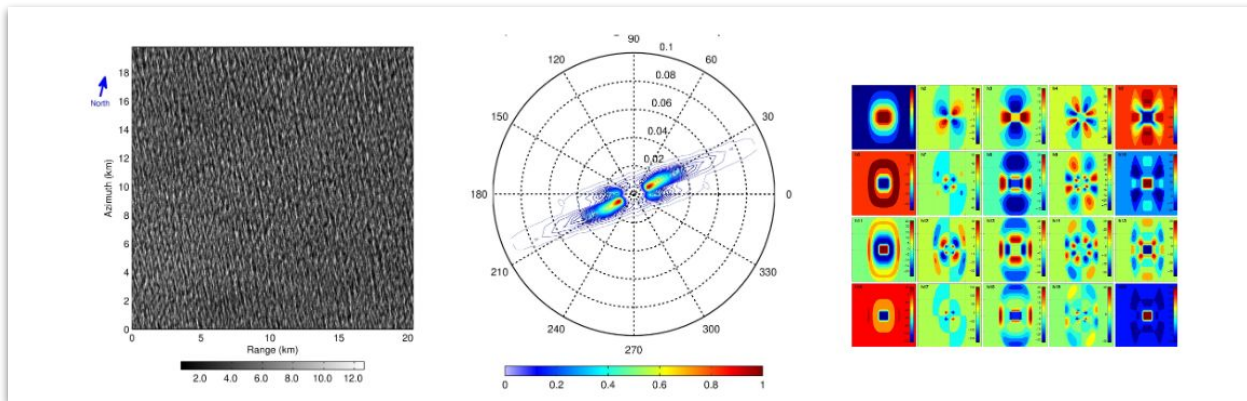
#### A. Sensors, Collocations and Preprocessing

Our first contribution is a data set of historical measurements from two types of polar-orbiting satellites: Sentinel-1 SAR satellites and altimetric satellites. Because the satellites are in different orbits, their paths intersect, providing

This algorithm has been published in IEEE TGRS in 2020.

The method aims at investigating the use of DL to start from X-spectra instead of using a predefined decomposition of the x-spectra (so-called CWAVE parameters).

This algorithm has been compared against other algorithms in the framework of CCI and proved to be better for Hs.



Example of Real part of X-spectra and the 20 parameters computed from the spectra for CWAVE

# SAR NN model to get Hs from WV cross spectra

Quach 2020 *et al* methodology described in this paper:

<https://authors.library.caltech.edu/104562/1/09143500.pdf>

Source datasets for NN model training:

1. Sentinel-1 WV L2 polar cross spectra + radar parameters
  2. Altimeter database from IMOS (Young *et al.*).
- CFOSAT SWIM measurement are not considered in the training dataset.**

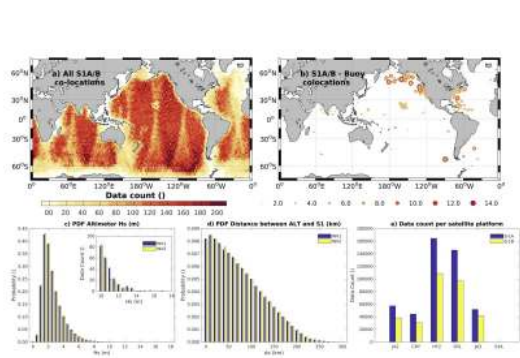


Fig. 1. Collocations between S-1 and satellite altimetry and moored buoys. (a) Total number of S-1/ALT collocations in  $2 \times 2^\circ$  bins. (b) Locations of the S-1/buoy collocations, the colors and size of the markers indicating the buoy  $H_s$ . (c) Histogram of  $H_s$  for S-1/ALT for WV1 and WV2, with the inset showing the tail for extreme sea states. (d) Histogram of distance between the S-1/ALT acquisitions for WV1 and WV2. (e) The graph showing number of collocations from each of the altimeter-SAR combinations.

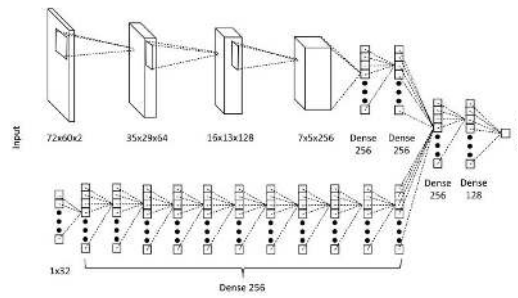


Fig. 3. DNN architecture with two input types. (Top) SAR image spect comprising one real and one imaginary channel. (Bottom) 32 scalar-value features. The SAR images are processed by multiple 2-D convolution layer before the two branches of the network are combined by three dense layers at the output. We predict  $H_s$  in this work, but we expect that the same model architecture could be used to predict other sea state parameters given an adequate training data set.

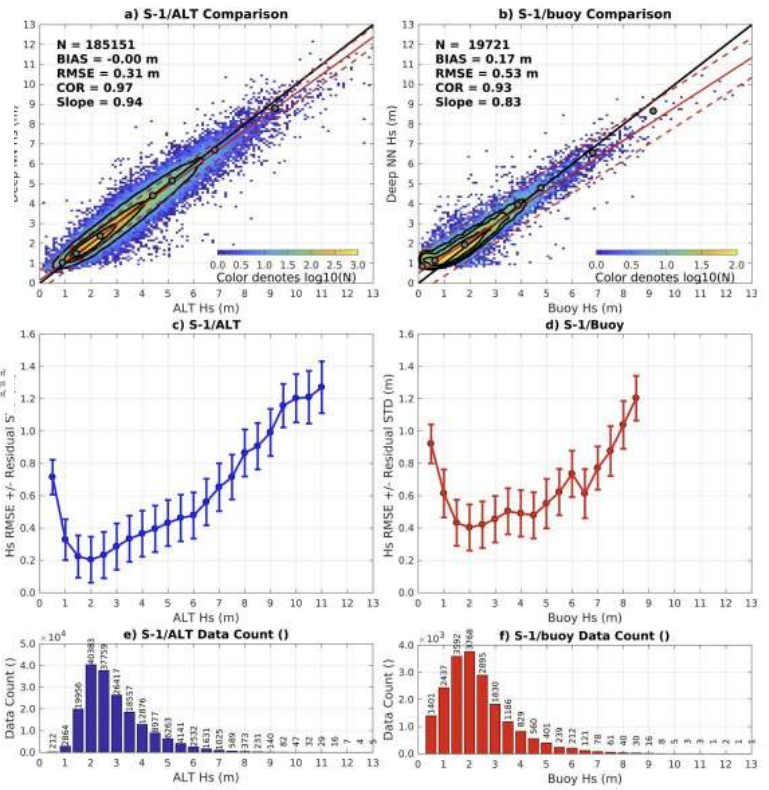
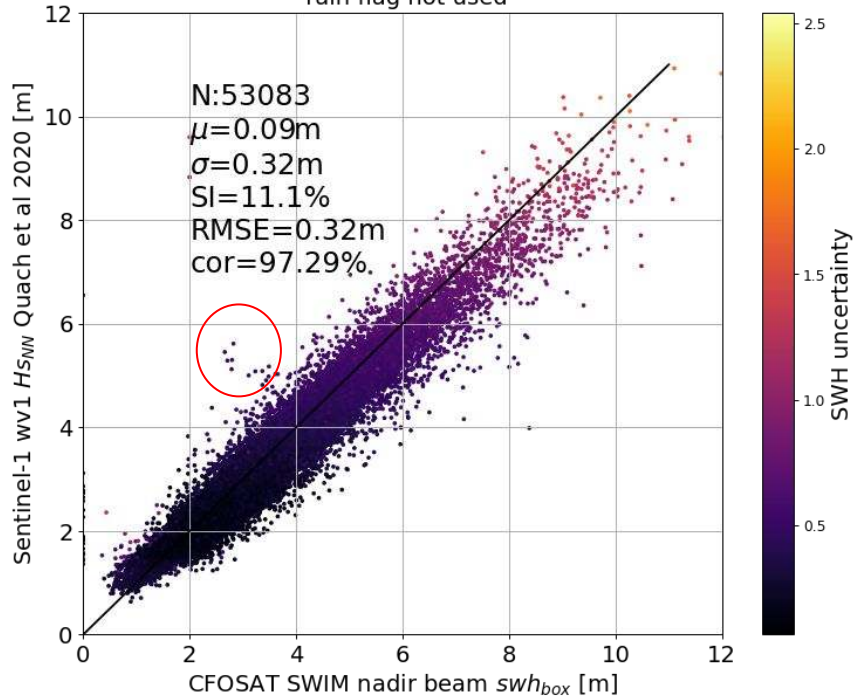


Fig. 7. Comparison of test predictions against (Left) altimeter collocations and (Right) buoy collocations. (a) and (b) Scatter plots of predictions versus measurements. (c) and (d) Plots of prediction RMSE vs measured  $H_s$ , with error bars showing the standard deviation. (e) and (f) Histograms of measured  $H_s$ , where the data count is given in black text. In the top panels, the color denotes data density in 0.1-m bins, solid red lines represent a least square linear regression, and the dashed lines represent 90% of the data. The black contours represent 50%, 75%, and 95% of the data (inner to outer) and the gray dots represent the quantile-quantile points for 1%, 10%, 50%, 90%, 95%, 99%, and 99.9%.

# Overall collocations Hs statistics

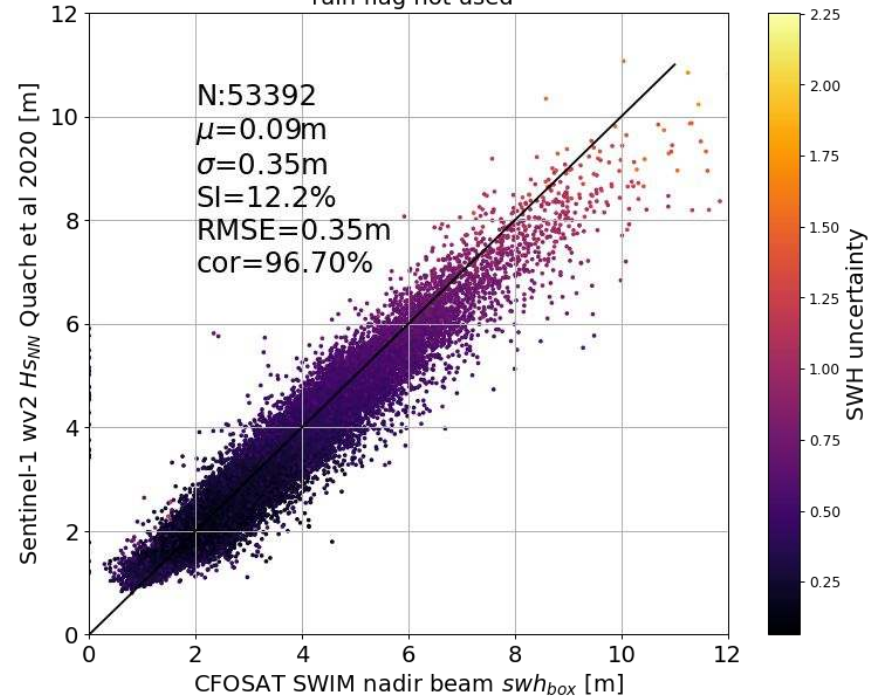
S1A wv1 Hs predictions versus SWIM

2019-04-01T01:11:23.000000000 2021-02-19T06:32:44.000000000  
rain flag not used



S1A wv2 Hs predictions versus SWIM

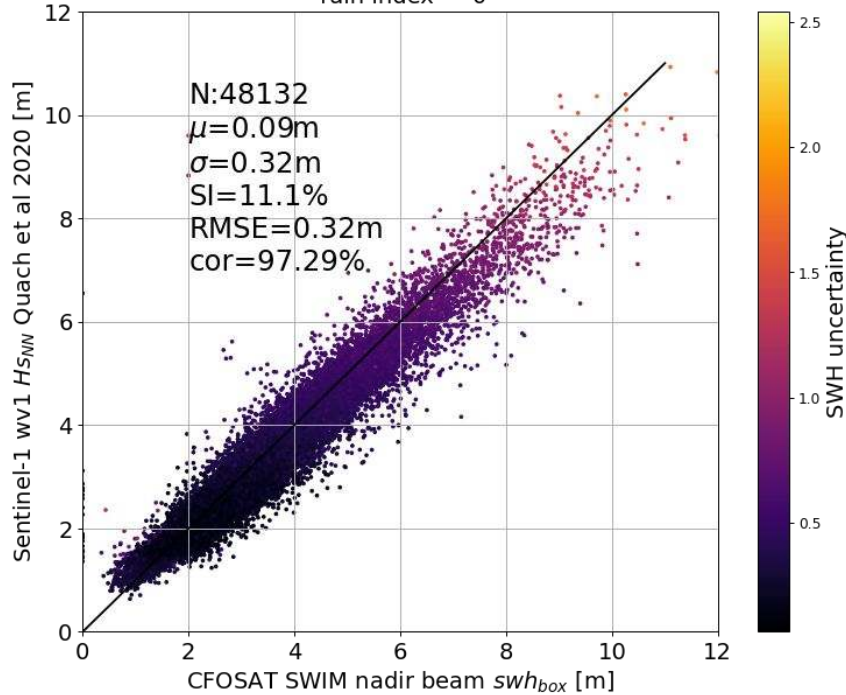
2019-04-01T02:55:57.000000000 2021-02-20T01:04:39.000000000  
rain flag not used



The Hs provided by NN model is associated to an uncertainty value. In Quach et al 2020 this uncertainty is the standard deviation of the difference between NN predictions and reference dataset. The 2 figures above are showing that this metric is directly linked with the Hs value but is not performant to detect anomalous observations-predictions.

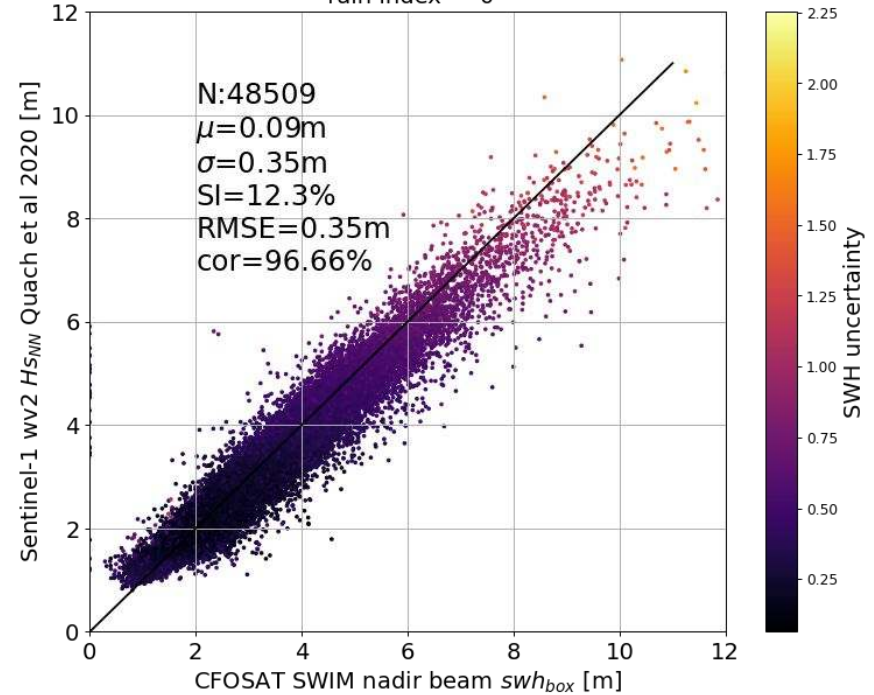
S1A wv1 Hs predictions versus SWIM

2019-04-01T01:11:23.000000000 2021-02-19T06:32:44.000000000  
rain index==0



S1A wv2 Hs predictions versus SWIM

2019-04-01T02:55:57.000000000 2021-02-20T01:04:39.000000000  
rain index==0

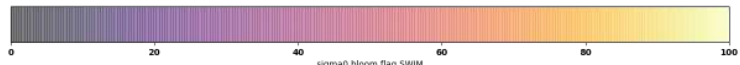
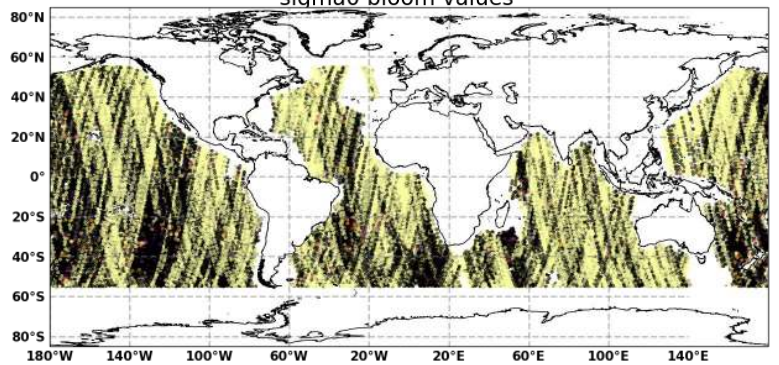
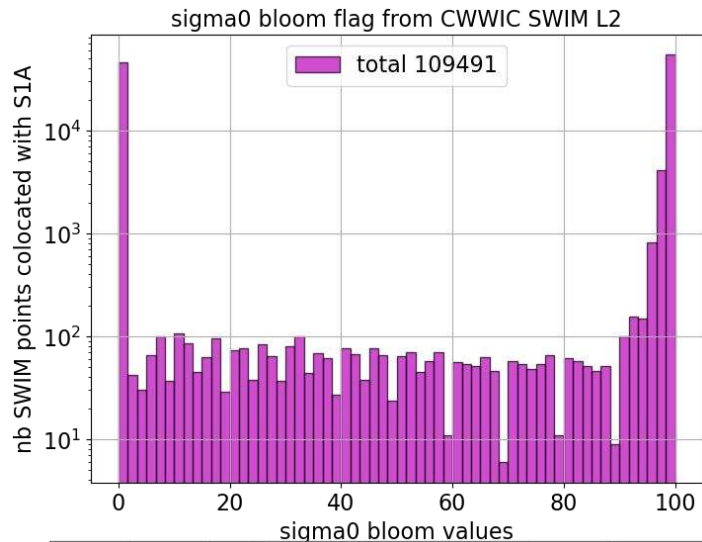


The rain flag provided by CWWIC in the L2 SWIM nadir product allows to remove some outliers. Overall, it doesn't change significantly the performances (even if it reduces by 16% the number of points). This could be a clue that this flag could be improved.

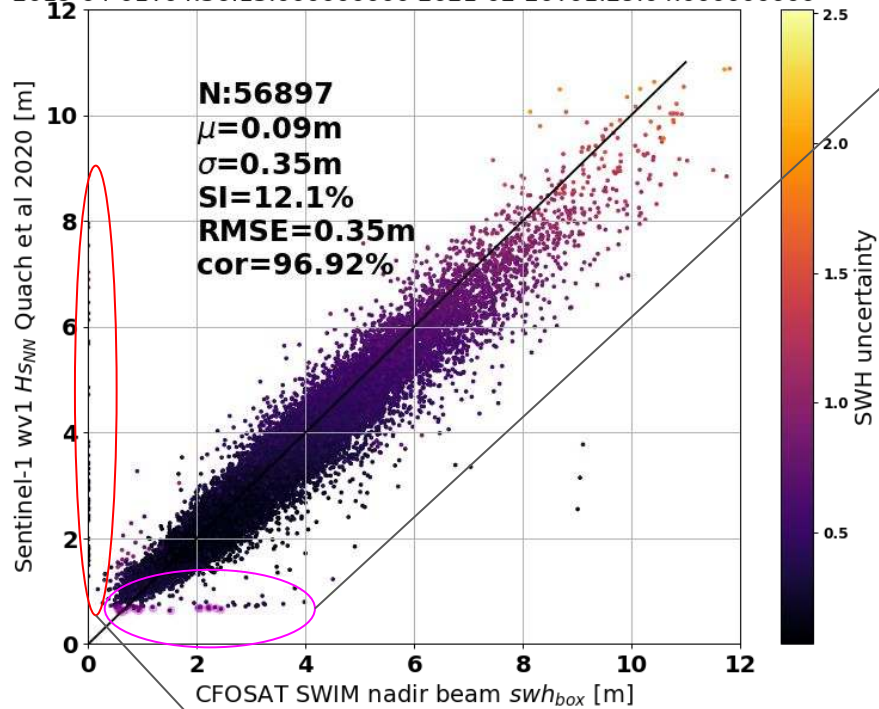
While the sigma0 bloom flag provided is not usable in the latest 5.1.2 version.

# SWIM sigma0 bloom flag

SWIM sigma0 bloom flag is designed to filter very low backscatter regions where the Hs retrieval using the altimeter waveforms is not possible or susceptible to be biased. The content of this flag is for now not usable because more than 50% of SWIM boxes are set to 100% bloom. The map is also showing no regional patterns but only full orbits flag with the same value.



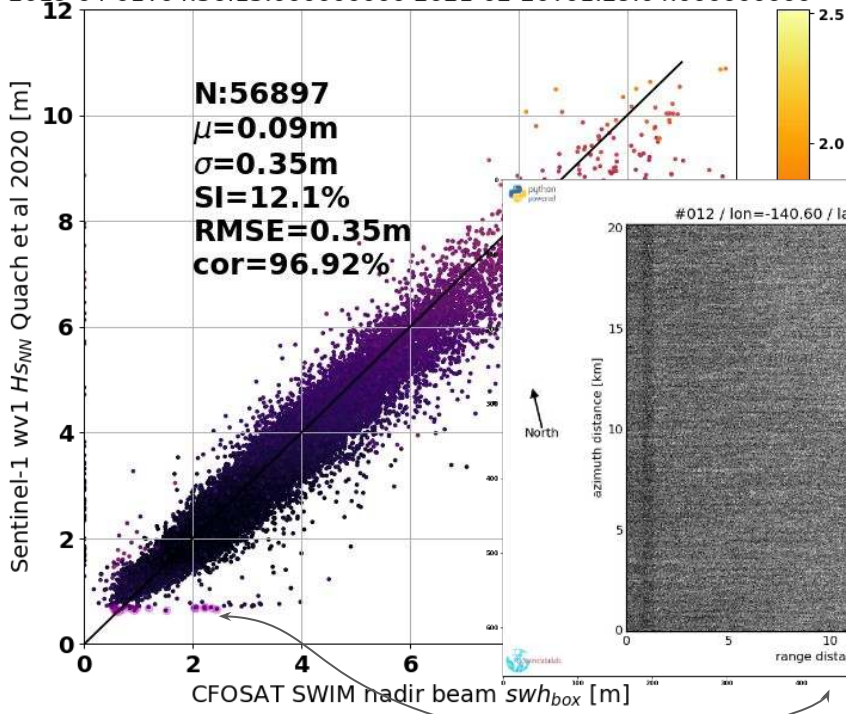
Validation CCI Sea State S-1 wv1 Hs predictions versus CFOSAT SWIM  
 2019-04-01T04:56:15.000000000 2021-02-20T01:29:04.000000000



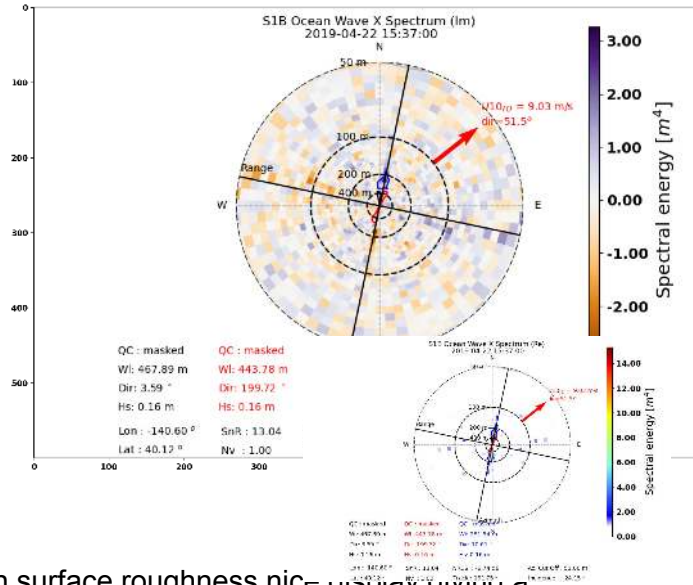
Focus on very low Hs predictions with Quach et al 2020 SAR algorithm.  
 Selection of 17 Sentinel-1 WV images with Hs < 0.7m

SWIM Hs = 0m are discussed slide 14.

Validation CCI Sea State S-1 wv1 Hs predictions versus CFOSAT SWIM  
 2019-04-01T04:56:15.000000000 2021-02-20T01:29:04.000000000

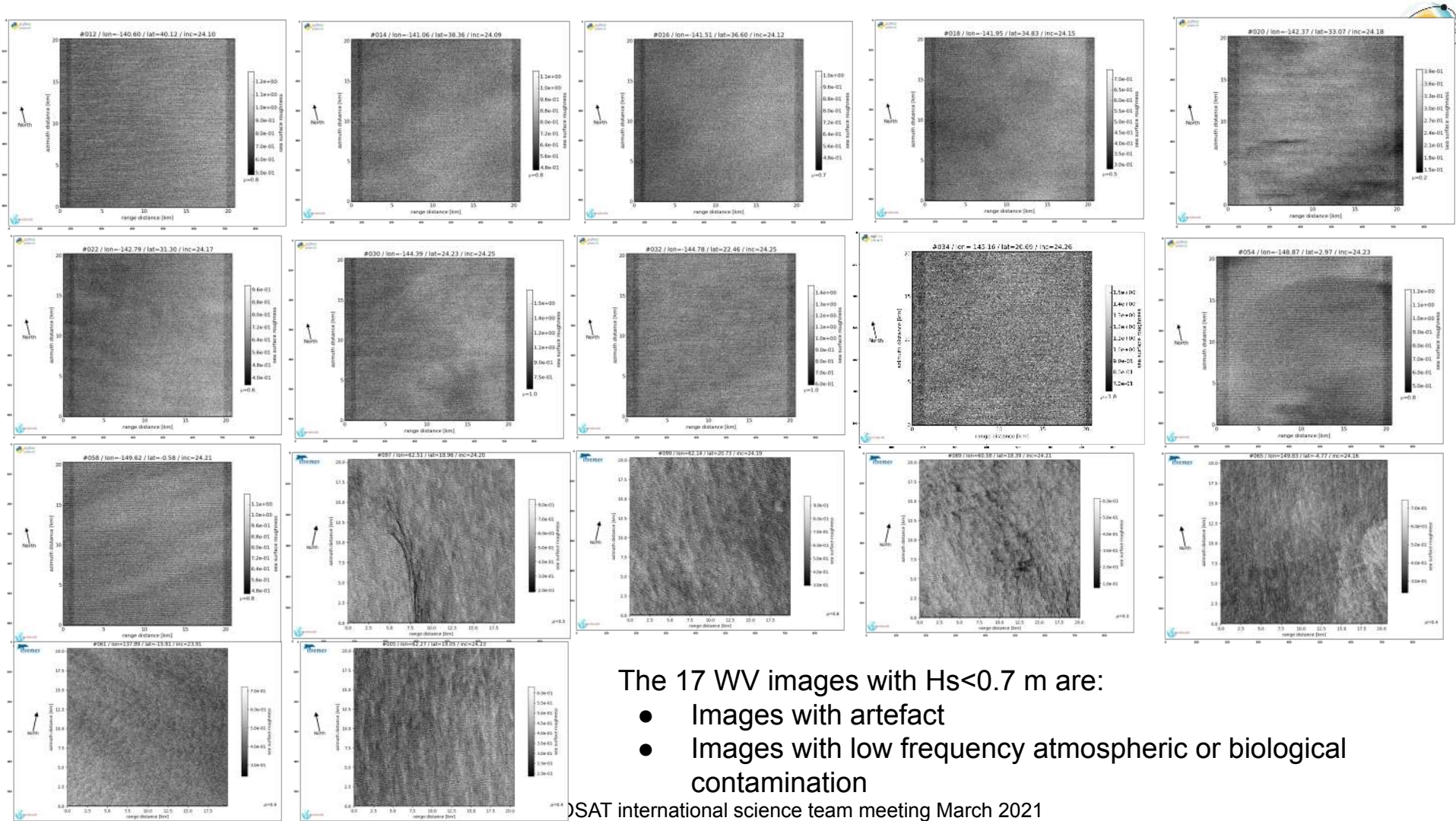


Focus on very low Hs predictions with Quach et al 2020 SAR algorithm.



Selection of 17 Sentinel-1 WV images with Hs < 0.7m

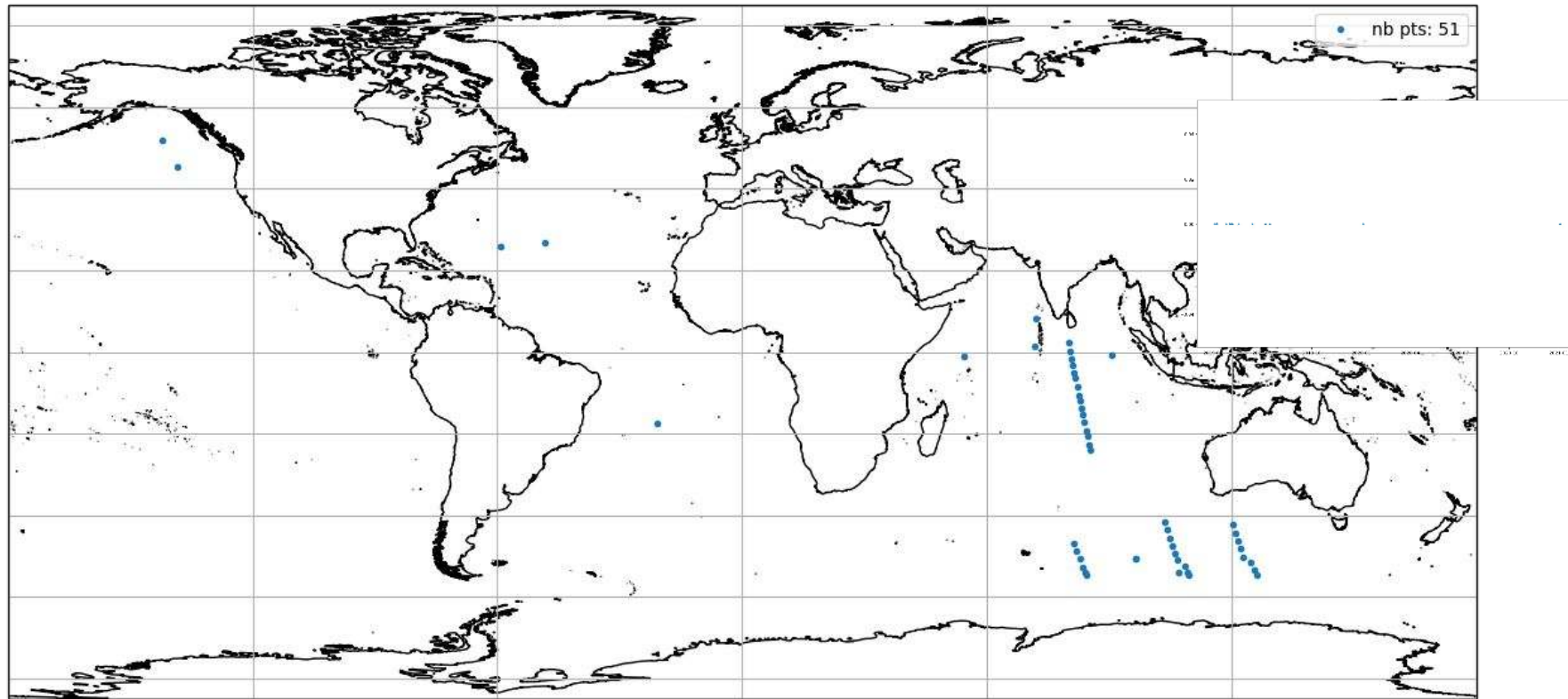
One example of the ocean surface roughness nice display giving a cross spectra with peak of energy along the azimuth axis and ultimately too low Hs. This image is showing vertical black lines that are artefacts impacting spectral Fourier transform and then Hs retrieval.



The 17 WV images with  $H_s < 0.7$  m are:

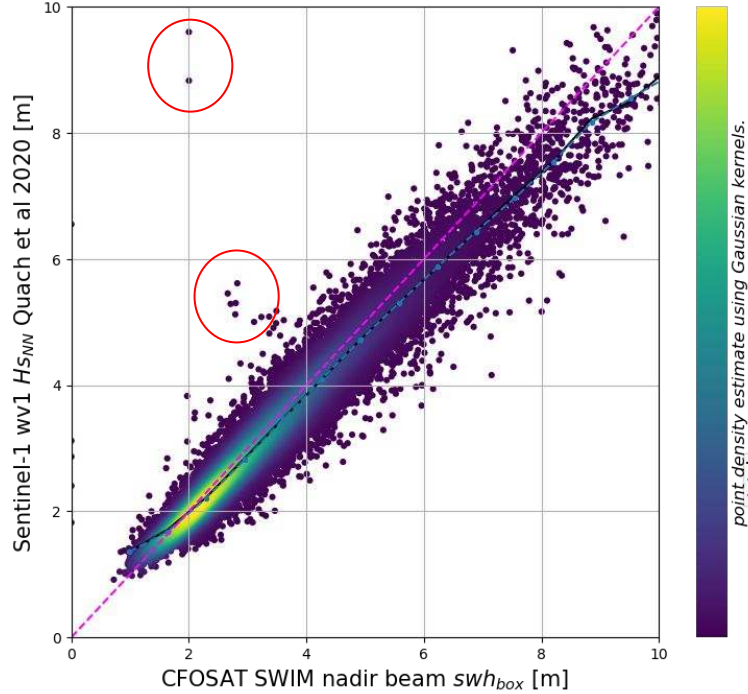
- Images with artefact
- Images with low frequency atmospheric or biological contamination

SWIM Hs = 0 m



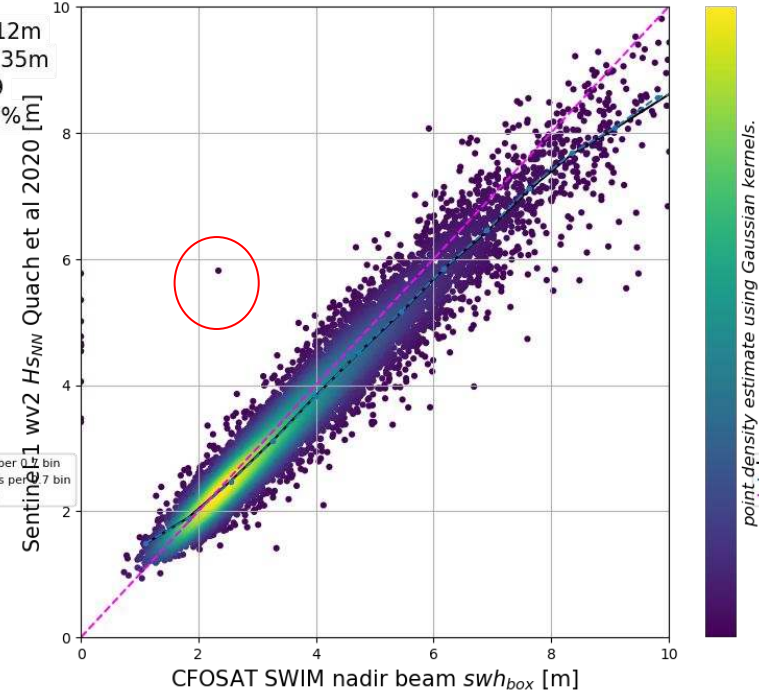
Few SWIM Hs are equal to zero m. They are located along same orbits at the beginning of the mission in 2019, it is very likely corrupted files.

S1Awv1 roughness class: POS Hs predictions vs SWIM  
 2019-04-01T01:11:23.000000000 2021-02-19T06:31:16.000000000



Bias: -0.12m  
 RMSE: 0.35m  
 N: 27009  
 SI: 10.32%  
 R: 0.97

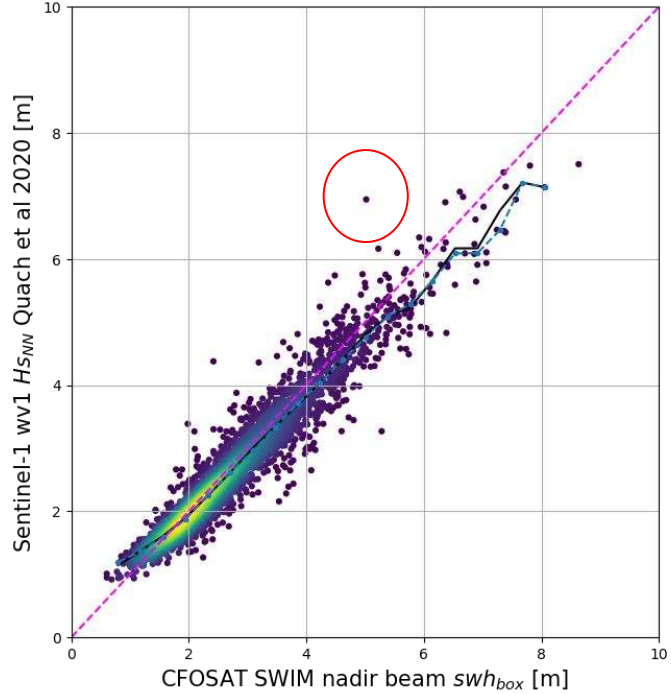
S1Awv2 roughness class: POS Hs predictions vs SWIM  
 2019-04-01T03:02:17.000000000 2021-02-19T01:36:14.000000000



Bias: -0.15m  
 RMSE: 0.44m  
 N: 10139  
 SI: 11.73%  
 R: 0.97

WV classified as “Pure Ocean Swell” by the Deep Learning algorithm developed by Chen et al 2018: <https://www.seanoe.org/data/00456/56796/>

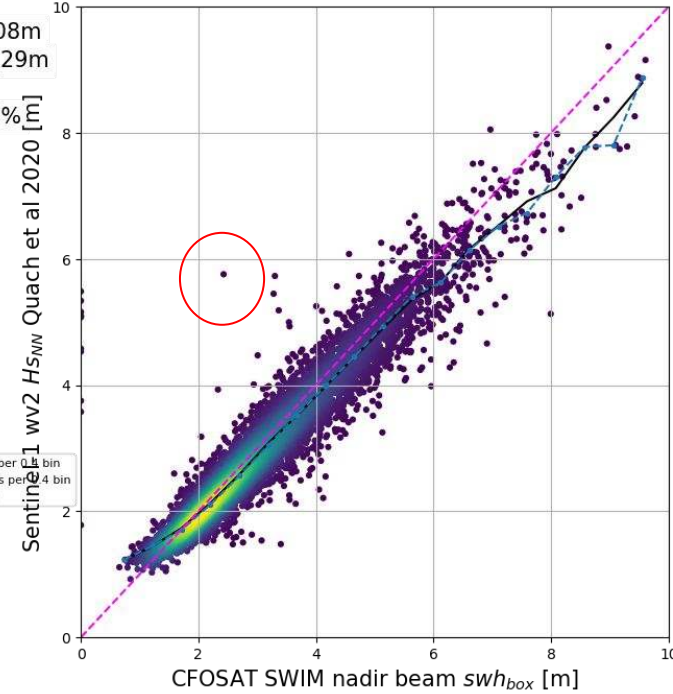
S1Aww1 roughness class:AF Hs predictions vs SWIM  
 2019-04-01T01:17:14.000000000 2021-02-19T06:30:18.000000000



Bias: -0.08m  
 RMSE: 0.29m  
 N: 3637  
 SI: 10.68%  
 R: 0.96

— mean Y values per 0.5 bin  
 — median Y values per 0.5 bin  
 - - orthogonal line

S1Aww2 roughness class:AF Hs predictions vs SWIM  
 2019-04-01T02:59:51.000000000 2021-02-19T01:35:16.000000000

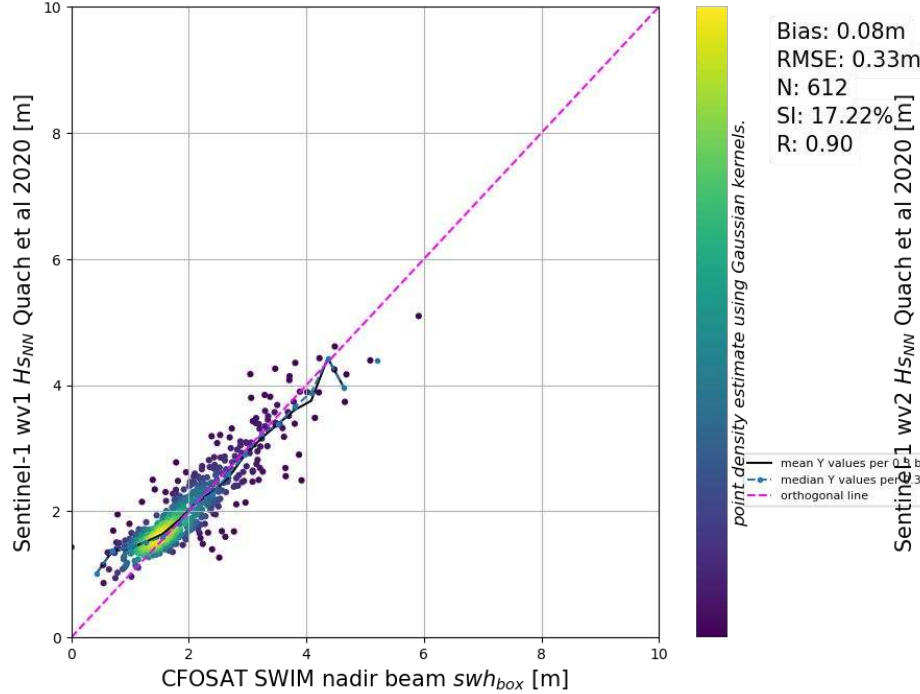


Bias: -0.10m  
 RMSE: 0.37m  
 N: 7426  
 SI: 12.17%  
 R: 0.96

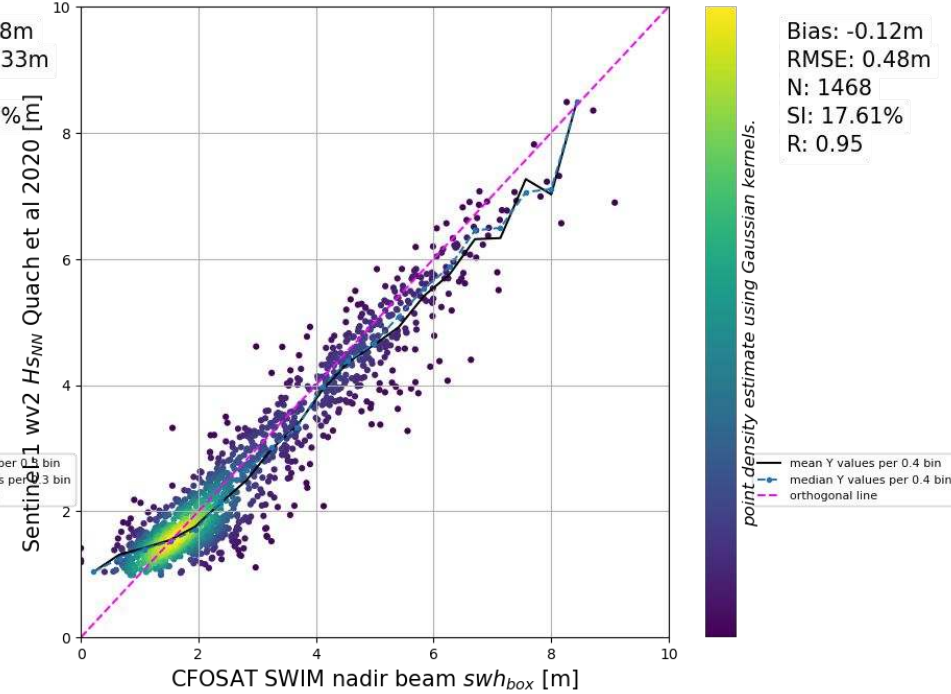
— mean Y values per 0.5 bin  
 — median Y values per 0.5 bin  
 - - orthogonal line

WV classified as “Atmospheric Front“ by the Deep Learning algorithm developed by Chen et al 2018: <https://www.seanoe.org/data/00456/56796/>

S1Awv1 roughness class:LWA Hs predictions vs SWIM  
 2019-04-01T02:58:08.000000000 2021-02-19T06:32:44.000000000

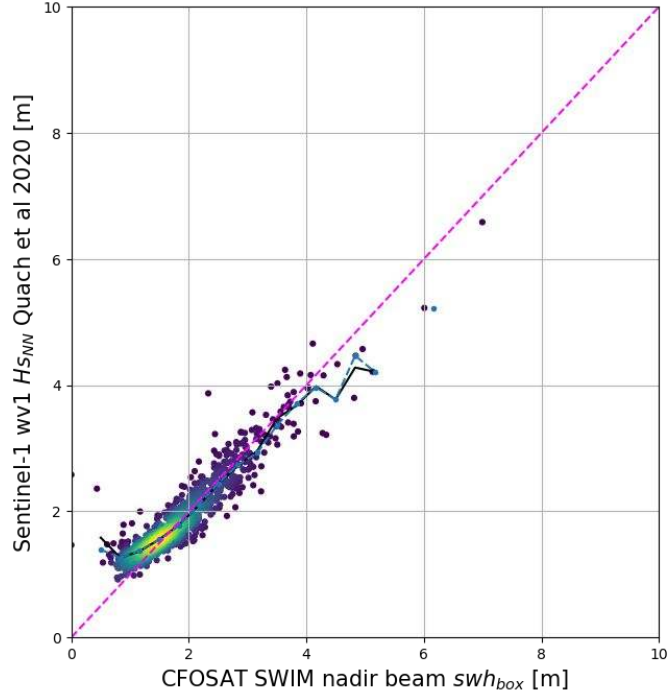


S1Awv2 roughness class:LWA Hs predictions vs SWIM  
 2019-04-01T02:57:54.000000000 2021-02-19T01:27:56.000000000



WV classified as “Low wind speed Area“ by the Deep Learning algorithm developed by Chen et al 2018: <https://www.seanoe.org/data/00456/56796/>

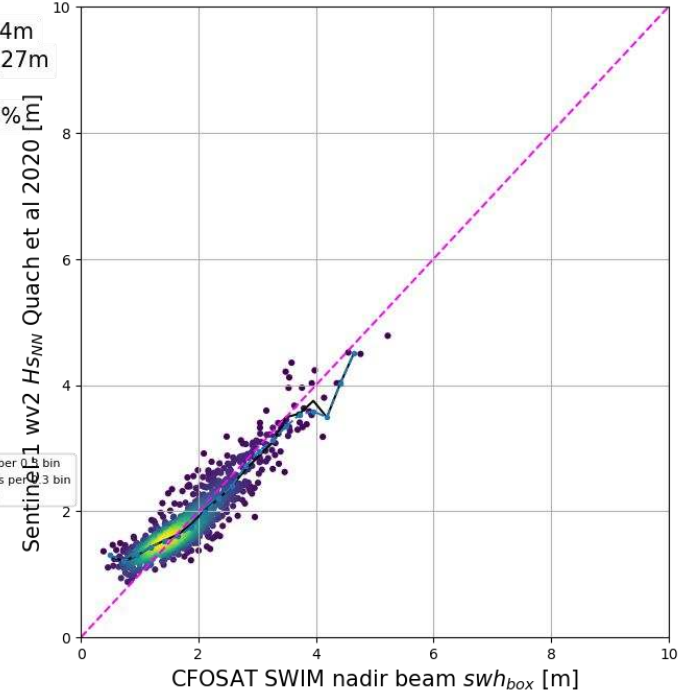
S1Aww1 roughness class:BS Hs predictions vs SWIM  
 2019-04-01T02:58:38.000000000 2021-02-19T06:32:15.000000000



Bias: 0.04m  
 RMSE: 0.27m  
 N: 1082  
 SI: 14.76%  
 R: 0.93

— mean Y values per 0.2 bin  
 — median Y values per 0.3 bin  
 - - - orthogonal line

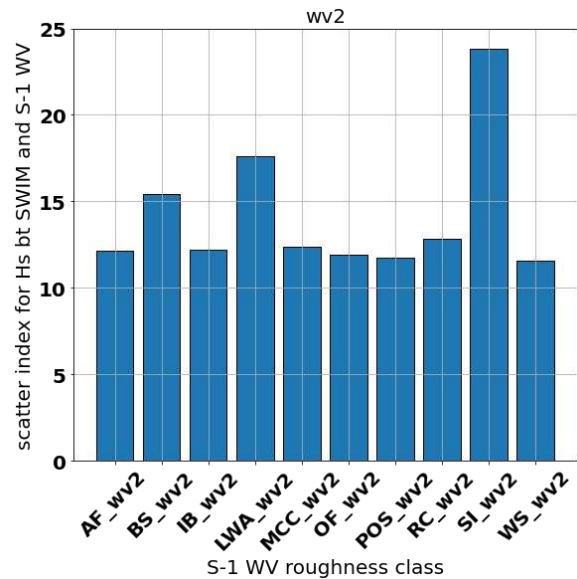
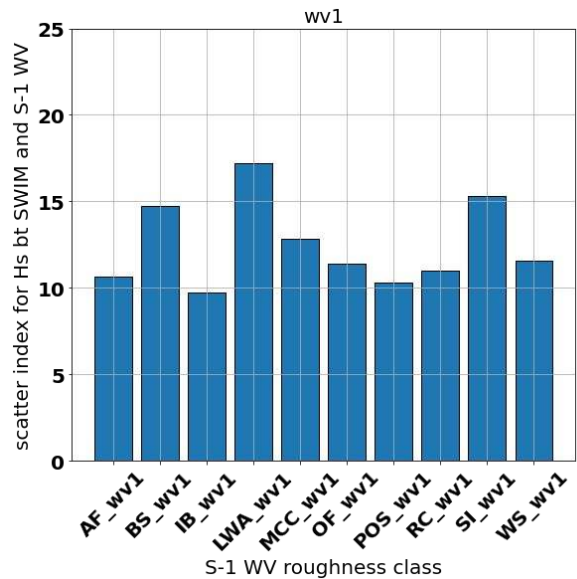
S1Aww2 roughness class:BS Hs predictions vs SWIM  
 2019-04-01T02:58:52.000000000 2021-02-17T08:09:04.000000000



Bias: 0.03m  
 RMSE: 0.28m  
 N: 983  
 SI: 15.45%  
 R: 0.91

— mean Y values per 0.2 bin  
 — median Y values per 0.2 bin  
 - - - orthogonal line

WV classified as “Biological Slicks“ by the Deep Learning algorithm developed by Chen et al 2018: <https://www.seanoe.org/data/00456/56796/>



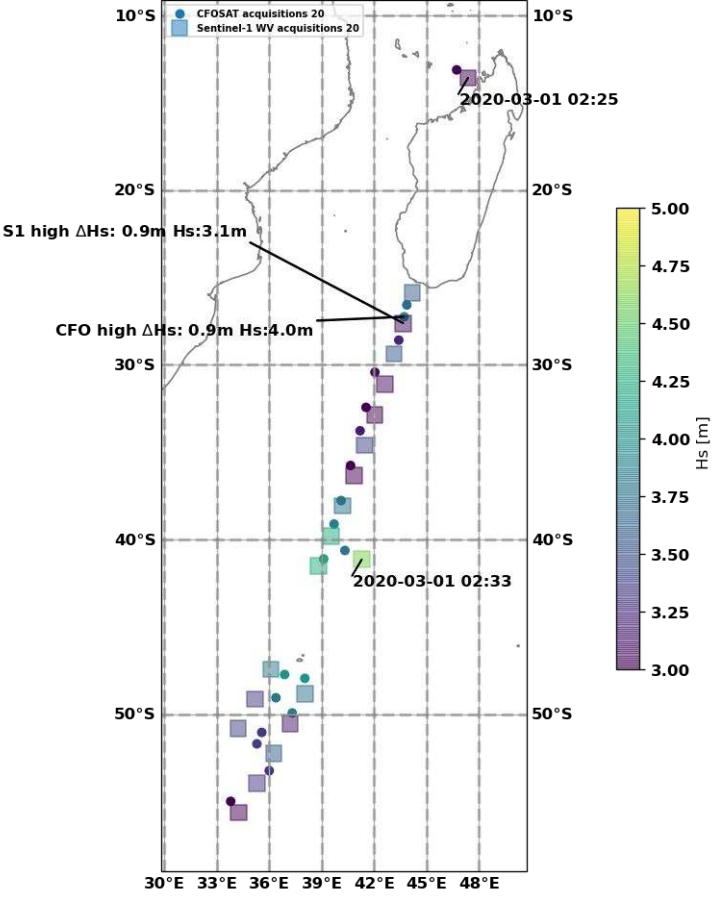
This figure is illustrating the fact that for some SAR images containing non wave geophysical features, the Hs retrieval is not giving the same performances. For instance we can see that the class SI (sea Ice) , or LWA (Low Wind Area) have scatter about ~40% higher than Pure Ocean Swell (POS).



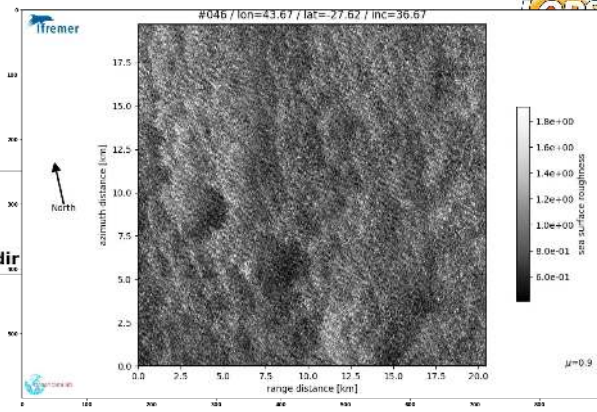
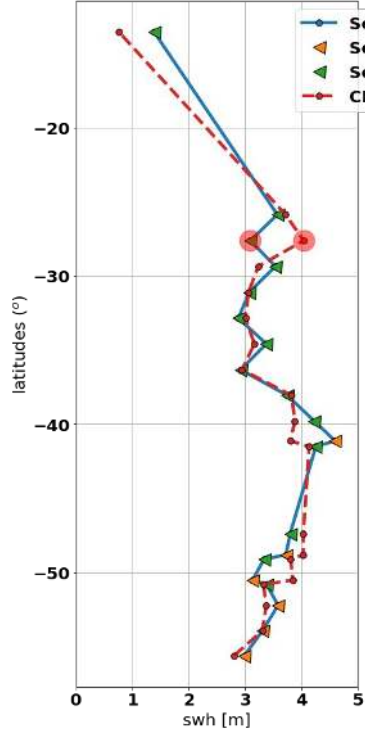
3 case studies to illustrate the performances of both products

# Example showing performances of the products along an orbit

SWIM & Sentinel-1 WV matchups  
 2020-03-01T01:29:30.000000000 - 2020-03-01T03:29:30.000000000  
 30°E 33°E 36°E 39°E 42°E 45°E 48°E



evolution of SWH along orbits  
 2020-03-01T01:29:30.000000000 - 2020-03-01T03:29:30.000000000

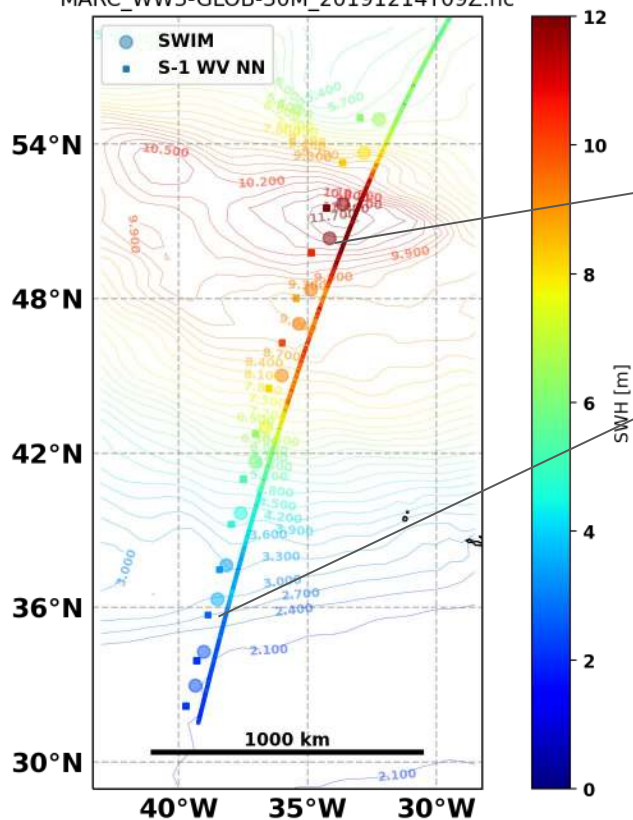


The Hs given by SWIM and Sentinel-1 are in good agreement for all the matchups along this orbit except for cases where the SAR image show the presence of rain cell (see surface roughness above).

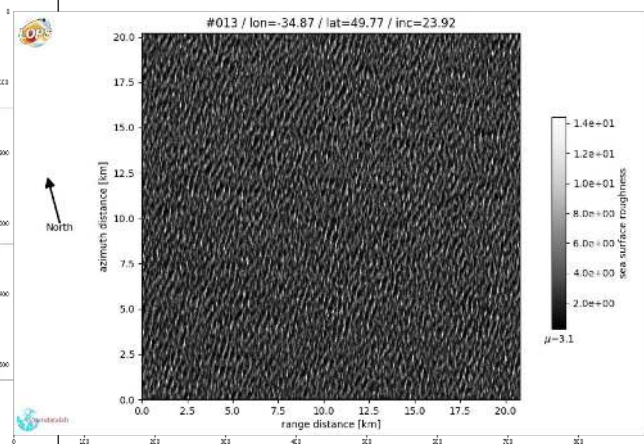
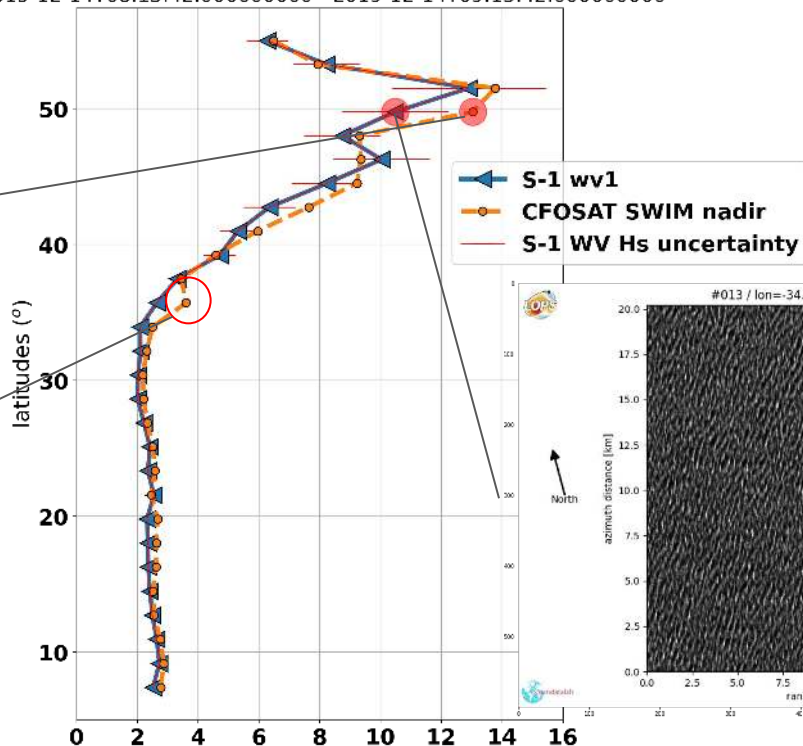
# Second case study with orbits crossing strong sea state region.



S1: 2019-12-14T08:43:42.000000000  
 SWIM: 2019-12-14T10:00:24.219548000  
 MARC\_WW3-GLOB-30M\_20191214T09Z.nc



evolution of SWH along orbits  
 2019-12-14T08:13:42.000000000 - 2019-12-14T09:13:42.000000000

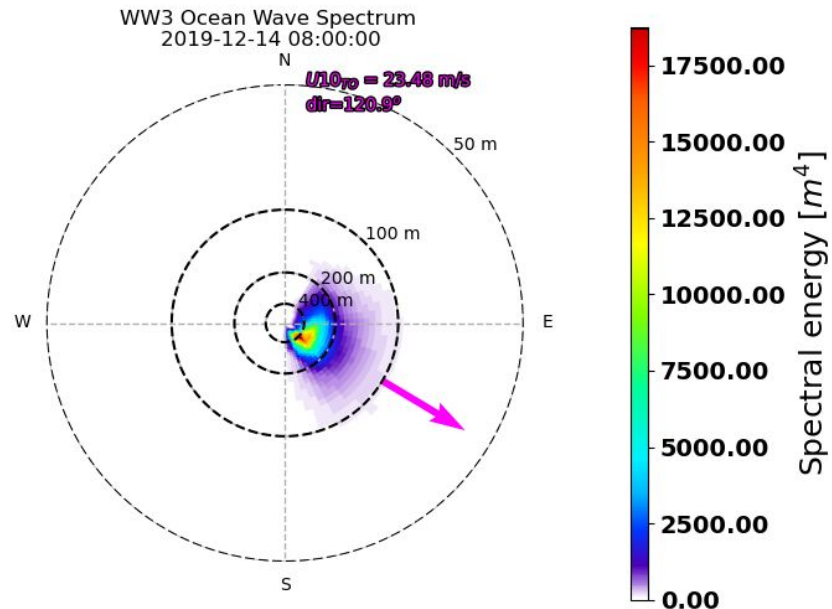
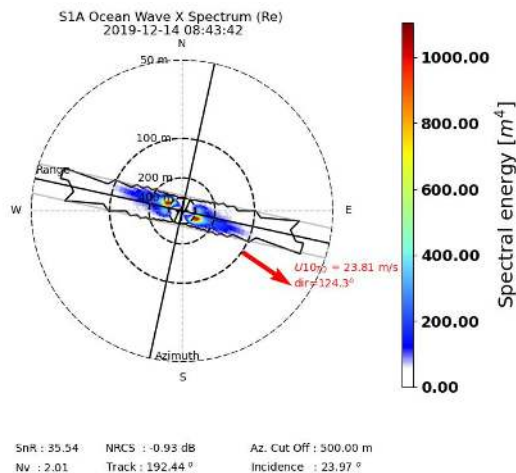
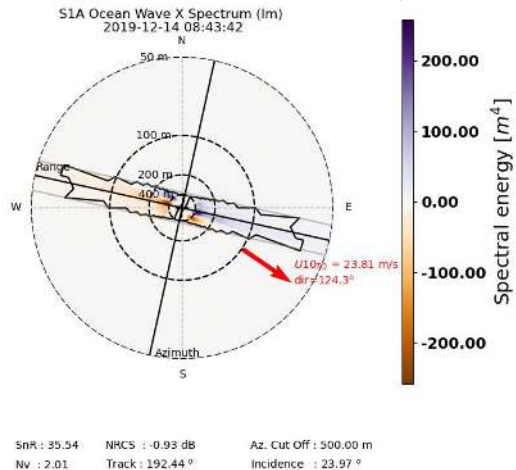


On this case with high Hs we selected the pair SWIM-S1 with the largest difference of Hs. The SAR image is not disturbed by low frequency contamination and the NN model gives a 11 m Hs while SWIM nadir beam is measuring 13 m. This is explained by the sharp sea state change within the 100km separating SWIM and the WV1.

# Second case study with orbits crossing strong sea state region.

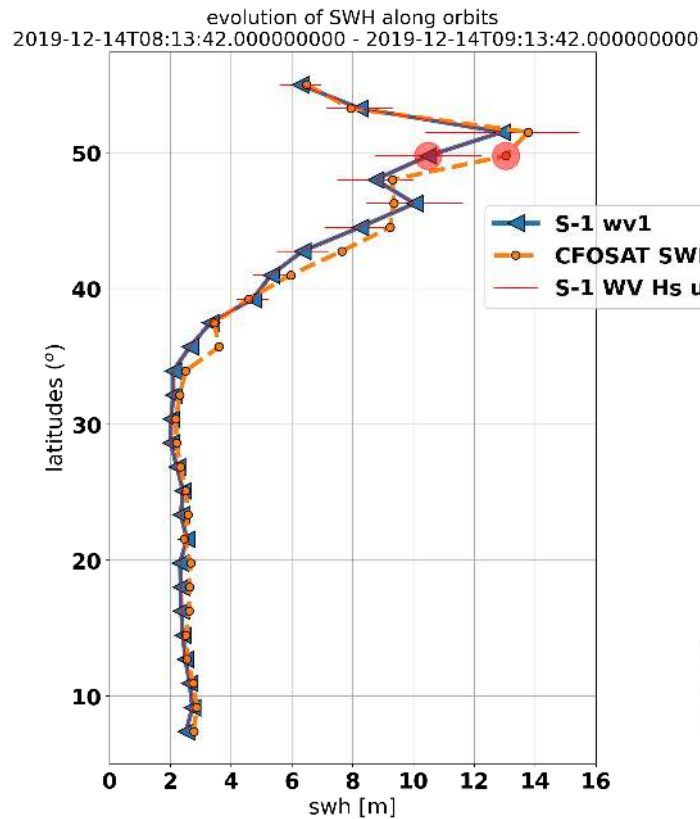
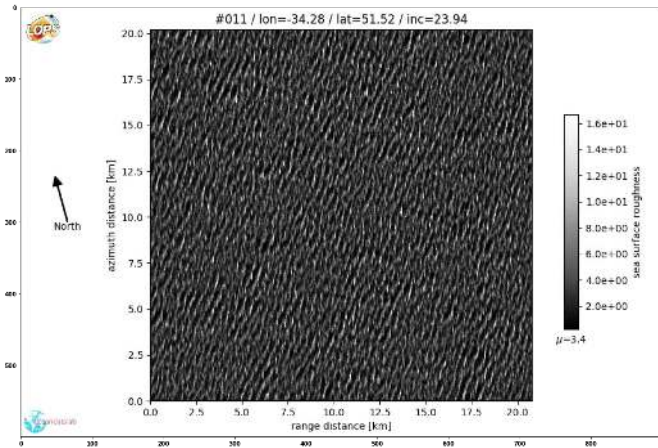


Cross Spectra (real and imaginary part) + WW3 wave height spectra associated to the suspect WV Hs.

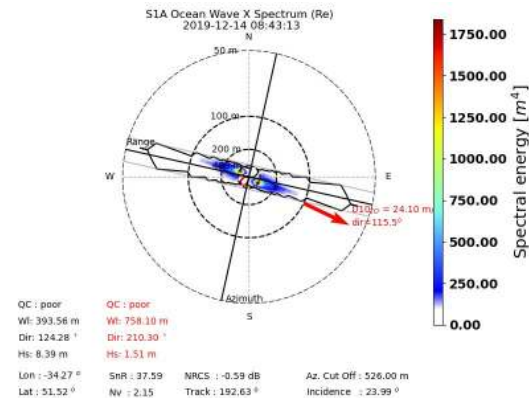


Lon : -35.00 °    Hs<sub>grid</sub> : 10.86 m  
Lat : 50.00 °

# Second case study with orbits crossing strong sea state region.



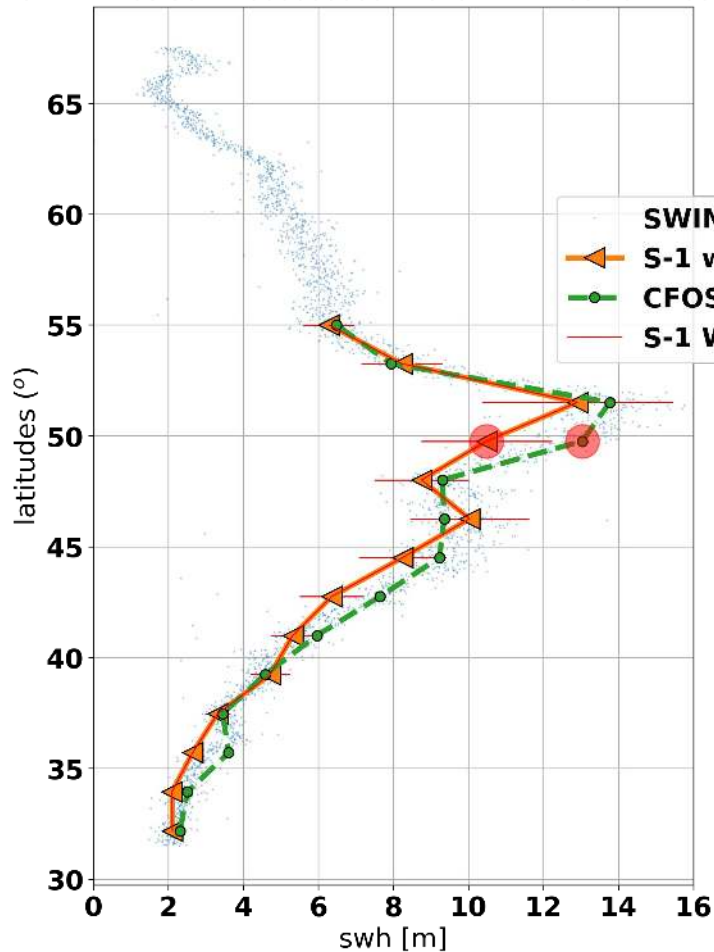
the WV1 just before (#011) 200 km North is in better agreement with SWIM while both products indicate higher Hs. It is simply due to the fact that this matchup has a closer spatial distance and less Hs gradient between the 2 points. This a very encouraging result to see that both products manage to provide Hs with less than 50cm difference within a 13-14m Hs.



# Second case study with orbits crossing strong sea state region.

evolution of SWH along orbits

2019-12-14T08:38:42.000000000 - 2019-12-14T08:48:42.000000000



The SWIM 5Hz is a bit noisy but most of the 5Hz points are within the uncertainty given by S-1 NN model.



This second case study shows that both products seem to give coherent Hs even in Hs above 12m. It also suggests that colocations between the 2 products should be done with smaller spatial distance. This could be achieved using the intermediate resolution product at 1 Hz for SWIM.



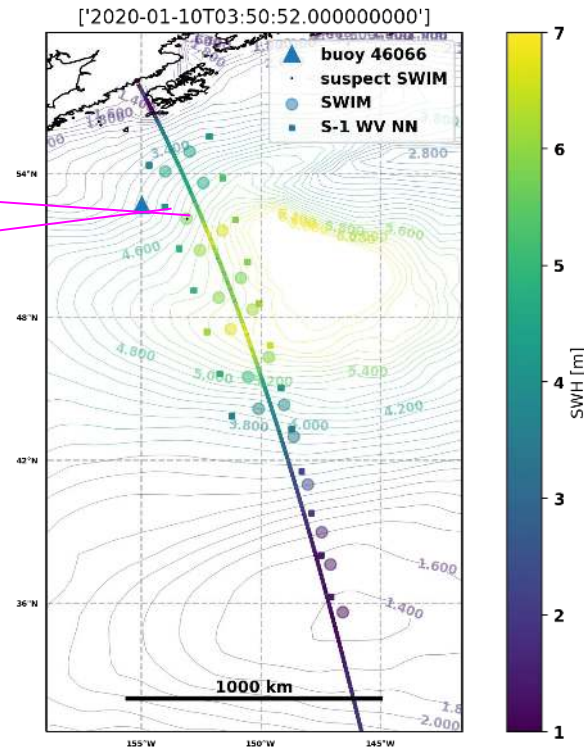
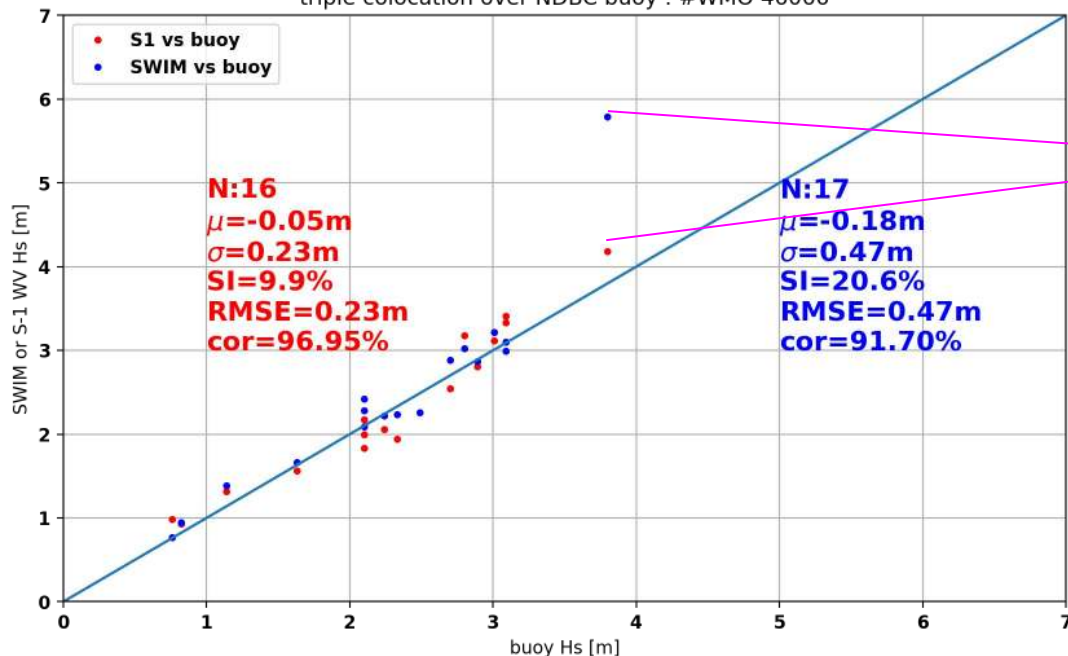
# Triple collocations (April 2019-now) over a buoy: SOUTH KODIAK - 310NM SSW of Kodiak, AK

On this example we can see that the SWIM have a point that is +1.8m above S-1 and the +2m wrt the buoy. The collocations is may be too loose on geographic criteria (100 km), while the time and space energy distribution within the 2 products seems coherent.

**WMO 46066**  
**Owned and maintained by National Data Buoy Center**  
**3-meter discus buoy**  
**SCOOP payload**  
**52.765 N 155.009 W (52°45'53" N 155° 0'32" W)**

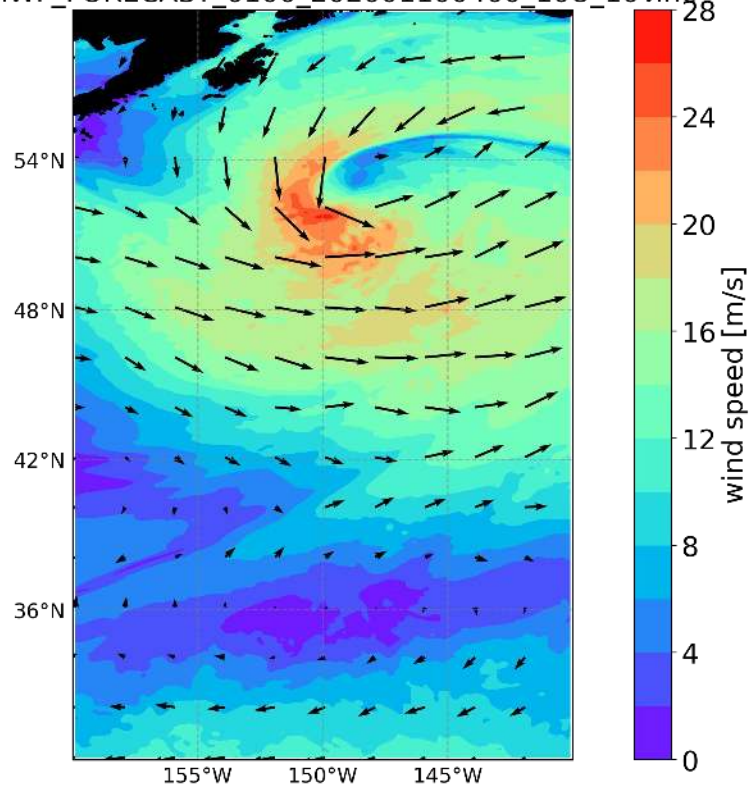


triple collocation over NDBC buoy : #WMO 46066

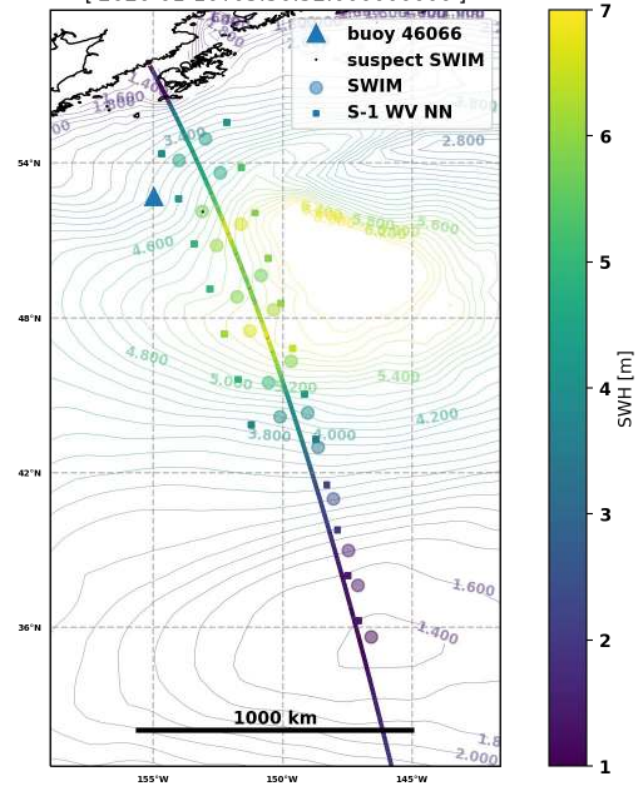


# Triple collocations (April 2019-now) over a buoy: SOUTH KODIAK - 310NM SSW of Kodiak, AK

ECMWF\_FORECAST\_0100\_202001100400\_10U\_10V.nc

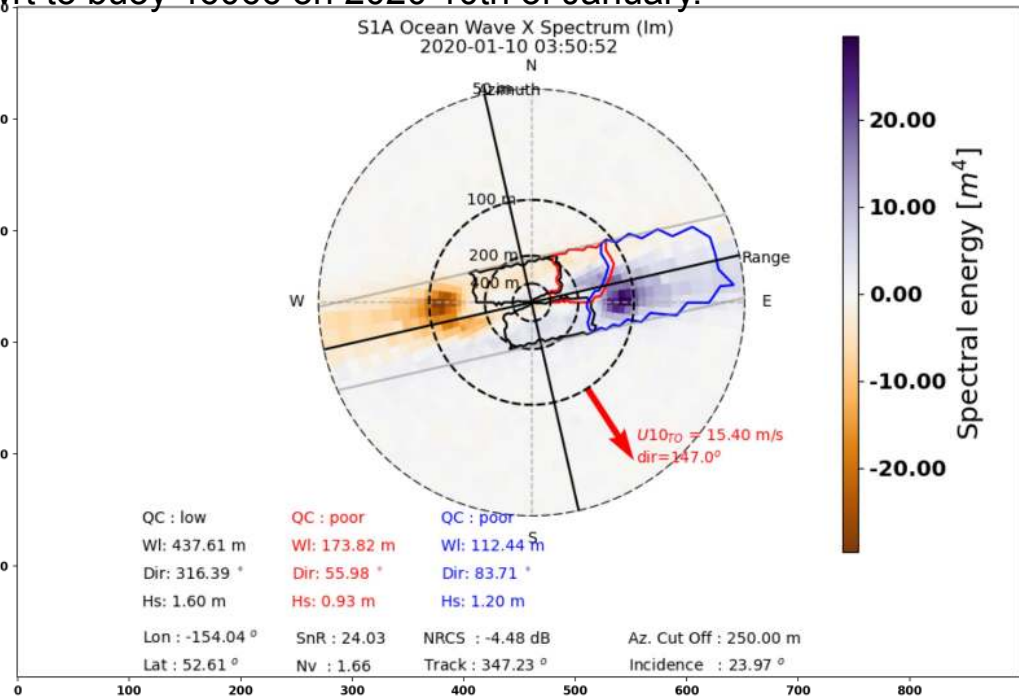
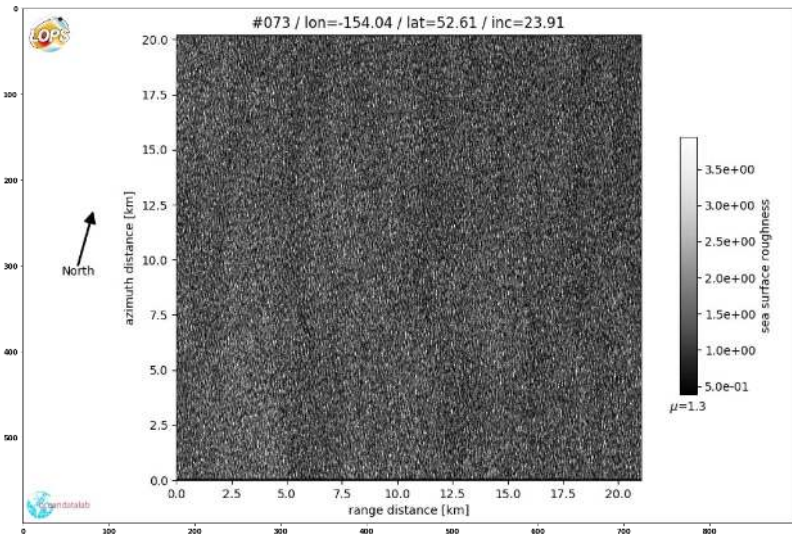


['2020-01-10T03:50:52.000000000']



# Triple collocations (April 2019-now) over a buoy: SOUTH KODIAK - 310NM SSW of Kodiak, AK

Illustration of the closest S-1 WV cross spectra wrt to buoy 46066 on 2020 10th of January.

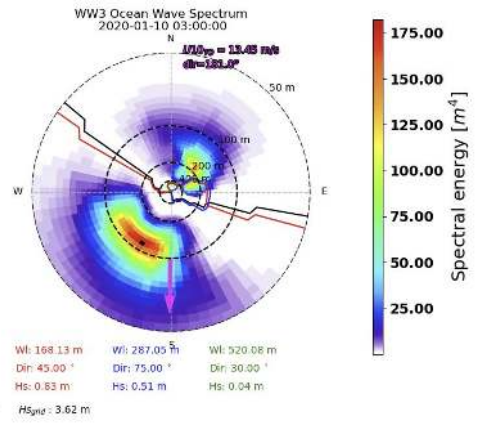
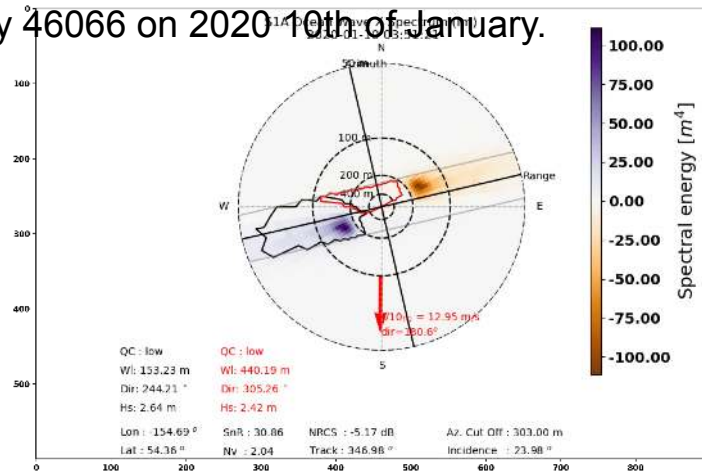
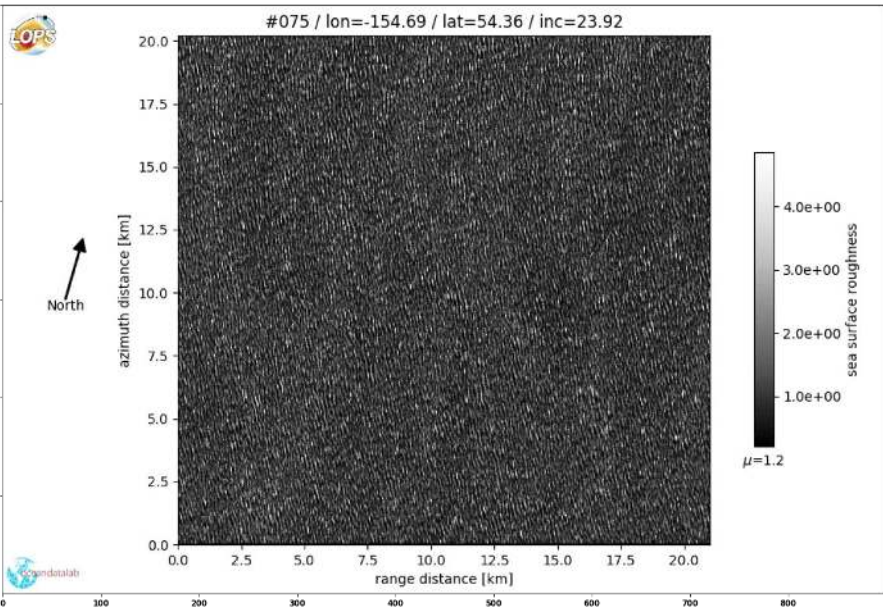


The main swell system dominated by the strong winds blowing to the East gives a quite clean SAR scene.

Triple collocations (April 2019-now) over a buoy:

**SOUTH KODIAK - 310NM SSW of Kodiak, AK**

Illustration of the closest S-1 WV cross spectra wrt to buoy 46066 on 2020 10th of January.



Few kilometers (~200km) to the North the same date, the swell system detected is totally different (storm coming from the North East).



## Conclusions

Independent estimates of Hs from CFOSAT (nadir beam) and Sentinel-1 (WV1 and WV2) acquisitions have been collocated and compared.

Overall the agreement between the two sensors is very good no matter Sentinel-1 acquisitions modes:

- WV1  $\mu=0.09\text{m}$   $\sigma=0.32\text{m}$
- WV2  $\mu=0.09\text{m}$   $\sigma=0.35\text{m}$

Surprisingly, the use of the rain flag as provided in CFOSAT (nadir beam) Level-2 product does not impact the results. However, the use of the SAR classification show that other geophysical phenomena (e.g. biological slicks) do impact the comparisons. The bloom flag as provided in CFOSAT (nadir beam) Level-2 product seems non-realistic.

Case study are also discussed. They confirm the ability of SAR and CFOSAT to capture the same sea state pattern at ocean basin scale. They also confirm the impact of geophysical phenomena such as rain on the comparisons.

A first attempt of triple collocation has been done on SOUTH KODIAK buoy. Overall it confirms the good consistency between SAR, CFOSAT and buoys:

- SAR-Buoy:  $\mu=-0.05\text{m}$   $\sigma=0.23\text{m}$
- CFOSAT-Buoy:  $\mu=-0.18\text{m}$   $\sigma=0.47\text{m}$

## Perspectives

Further investigation are necessary to assess the impact of the other geophysical phenomena on CFOSAT and possibly help to refine the bloom flag and the potential/limitations of both missions in case of extremes.

The validation of the directional and wavelength information between the two sensors needs also to be pursued.



Thank you for reading, we are ready to answer your questions.